Please cite the Published Version

Saczek, Joshua, Jamieson, Oliver, McClements, Jake , Dann, Amy, Johnson, Rhiannon E, Stokes, Alexander D, Crapnell, Robert D, Banks, Craig E, Canfarotta, Francesco, Spyridopoulos, Ioakim, Thomson, Alan, Zaman, Azfar , Novakovic, Katarina and Peeters, Marloes (2025) Troponin I Biomarker Sensing from Clinical Patient Samples using Molecularly Imprinted Polymer Nanoparticles for Advancing Healthcare Approaches in Cardiovascular Disease. Biosensors and Bioelectronics, 282. 117467 ISSN 0956-5663

DOI: https://doi.org/10.1016/j.bios.2025.117467

Publisher: Elsevier

Version: Published Version

Downloaded from: https://e-space.mmu.ac.uk/639492/

Usage rights: Creative Commons: Attribution 4.0

Additional Information: This is an open access article published in Biosensors and Bioelectron-

ics, by Elsevier.

Data Access Statement: Data will be made available on request.

Enquiries:

If you have questions about this document, contact openresearch@mmu.ac.uk. Please include the URL of the record in e-space. If you believe that your, or a third party's rights have been compromised through this document please see our Take Down policy (available from https://www.mmu.ac.uk/library/using-the-library/policies-and-guidelines)

\$ SUPER

Contents lists available at ScienceDirect

Biosensors and Bioelectronics

journal homepage: www.elsevier.com/locate/bios





Troponin I biomarker sensing from clinical patient samples using molecularly imprinted polymer nanoparticles for advancing healthcare approaches in cardiovascular disease

Joshua Saczek ^{a,b}, Oliver Jamieson ^{a,b}, Jake McClements ^a, Amy Dann ^{a,b}, Rhiannon E. Johnson ^c, Alexander D. Stokes ^a, Robert D. Crapnell ^d, Craig E. Banks ^d, Francesco Canfarotta ^c, Ioakim Spyridopoulos ^e, Alan Thomson ^c, Azfar Zaman ^e, Katarina Novakovic ^a, Marloes Peeters ^{a,b,*}

- ^a Newcastle University, School of Engineering, Merz Court, Claremont Road, NE1 7RU, Newcastle Upon Tyne, UK
- ^b School of Engineering, Engineering A building, East Booth Street, University of Manchester, M13 9QS, Manchester, UK
- ^c MIP Discovery Ltd, The Exchange Building, Colworth Park, Sharnbrook, MK44 1LQ, Bedford, UK
- ^d Manchester Metropolitan University, Faculty of Science and Engineering, Chester Street, M1 5GD, Manchester, UK
- e Department of Cardiology, Freeman Hospital and Newcastle University, Translational and Clinical Research Institute, NE7 7DN, Newcastle upon Tyne, UK

ARTICLE INFO

Keywords: Molecularly imprinted polymer nanoparticles (NanoMIPs) Biosensors Troponin I (cTnI) Myocardial infarction Cardiovascular disease

ABSTRACT

Cardiac troponin I (cTnI) is a critical protein biomarker for heart attack diagnosis. This study presents a thorough analysis of a novel biosensing device utilizing molecularly imprinted polymer nanoparticles (nanoMIPs) for detecting cTnI in clinical patient serum samples post myocardial infarction. The methodology, based on the heat-transfer method approach, offers faster measurements times than the current gold standard and sample volumes equivalent to a single blood drop. Biomarker binding shows performance comparable to a high-sensitivity ELISA, accurately identifying patients with elevated cTnI levels ($R^2=0.893$). The cTnI peak concentration time variations are attributed to heterogeneous serum complexes, with different troponin complex sizes potentially generating differing thermal insulation levels. Comparison with an established patient database demonstrates robust correlations between our cTnI concentrations and clinical parameters ($R^2=0.855$). This underscores the potential of nanoMIP sensors for sensitive cTnI detection, providing insights into post-heart attack biomarker levels. Furthermore, our methodology presents the additional benefits of being low cost and portable enabling measurements at time and place of patients. Consequently, it holds the potential to become a vital part of the diagnostic pathway for heart attack treatment, ultimately reducing healthcare costs and improving patient outcomes.

1. Introduction

Within the UK, \sim 7.6 million people are living with cardiovascular diseases (CVDs), and 25 % of all UK deaths are attributed to CVD, resulting in healthcare costs of \sim £9 billion each year (Foundation, 2023a). Similar findings are present within the rest of Europe and the USA, with CVD being responsible for 45 % and 25 % of all deaths, respectively, demonstrating the global scale of the issue (Wilkins et al., 2017; Benjamin et al., 2017). Furthermore, since the SARS-CoV-2 pandemic, deaths involving CVD within the UK have risen above expected levels, with a particular uptick in cases of acute myocardial

infarction (MI) in young people (<45 years old) (Foundation, 2023b; Xie et al., 2022). CVD describes multiple disorders that affect the heart and circulatory system. This work focuses on MI, otherwise known as heart attacks, as it has the highest morbidity and mortality rate (Ojha et al., 2023; Sacco et al., 2013; Henderson, 1996). MI occurs when heart tissue is damaged, leading to a state of hypoxia and eventual ischemia and myocyte necrosis (Park et al., 2017). When muscles within the heart sustain damage, unique cardiac proteins are released into the blood-stream, including cardiac troponin I and T (cTnI and cTnT). The severity of this damage can be quantified by measuring cardiac troponin's highly

^{*} Corresponding author. Newcastle University, School of Engineering, Merz Court, Claremont Road, NE1 7RU, Newcastle Upon Tyne, UK. *E-mail address:* marloes.peeters@manchester.ac.uk (M. Peeters).

specific and sensitive nature (Gaze et al., 2008; Crapnell et al., 2022). To further aid diagnostic and prognostic decision-making, troponin measurements are often combined with other clinical assessment methods, such as electro/echocardiograms, and knowledge of family history and preexisting health conditions (Pickering et al., 2017; Barrett-Connor et al., 1984).

Of the ~700,000 individuals who attend accident and emergency (A&E) due to chest pain each year in the UK, >75 % are not experiencing a MI (Stepinska et al., 2020; Cross et al., 2007). The number of beds occupied by patients who are admitted on this basis but are then not diagnosed with MI is placing additional pressure on the already overstretched National Health Service in the UK, with similar trends occurring globally (Capewell et al., 2000; Nadarajah et al., 2023; Thomas et al., 2020). In a study by Zhou et al., it is discussed that patients with a previously diagnosed cardiovascular disease (CVD) incur significantly higher healthcare costs—approximately double—compared to patients without a prior CVD diagnosis, highlighting the critical need for improved initial myocardial infarction (MI) diagnosis (Zhou et al., 2023). The current diagnostic "gold standard" test for MI utilizes immunoassays, more specifically enzyme-linked immunosorbent assays (ELISAs), primarily focusing on cTnI or cTnT, with a typical limit of detection (LoD) around 1 ng L^{-1} (Guidance, 2020). However, the selected analyte can produce significantly different responses, with assays utilizing differing epitopes, which makes direct comparisons difficult (Guy et al., 2013). Moreover, their high cost, attributed to the necessity of using specific equipment in a laboratory setting and employing antibodies as recognition elements, along with extended turnaround times (1-3 h), poses significant limitations (Lippi et al., 2013). Measurement time is particularly critical as mortality is closely linked with time to MI diagnosis, where treatment within the "golden hour" can reverse damage to the heart muscles (Boersma et al., 1996). This time constraint is unavoidable with current ELISAs, which require processing in the hospital's laboratory by trained personnel rather than being performed at the patient's bedside (Hornbeck, 2015).

Due to these limitations generated through the use of ELISA in the standard hospital pathways for MI diagnosis, alternative sensor platforms, such as nanoparticle-based or optical systems, have been developed (Wang et al., 2023; Zhan et al., 2022a). However, these alternatives require expensive materials, complex equipment, and face performance challenges, including light fluctuation interference and reliance on specialized cells and electrodes (Shumyantseva et al., 2018). Our nanoMIP-based approach is cost-effective, robust, and easy to synthesize, making it more suitable for widespread use than other ELISA alternatives, especially in low-resource settings. Furthermore, enzyme-based or fluorescent probe biosensors degrade over time, compromising reliability and requiring frequent recalibration (Zhan et al., 2022a). NanoMIPs offer superior stability and durability, maintaining integrity even under harsh conditions.

Introducing a rapid MI rule-out test for A&E using cTnI measurements alongside existing healthcare pathways could help alleviate healthcare burdens and significantly improve patient outcomes (Foundation, 2023b; Ghilencea et al., 2022). Multiple alternative avenues are being considered to traditional immunoassays, such as electrochemical and infrared spectrophotometric sensing (Gao et al., 2024; Sengupta et al., 2023). To overcome the limitations of immunoassays, we propose the replacement of antibodies with molecularly imprinted polymer nanoparticles (nanoMIPs), which are polymeric recognition elements that rival the affinity of antibodies (Sharma et al., 2004; Haupt et al., 1998). Furthermore, they are highly versatile, adaptable to detect almost any target of interest, whilst offering extreme stability as they do not require fridge storage and show extended shelf life.

NanoMIPs offer an alternate and clinically viable solution to cTnI sensing due to their inherent physical and operational stability alongside their expeditious binding capabilities (Choudhary et al., 2023). Work by McClements et al. considered various approaches to best utilize nano-MIPs for the ultrasensitive detection of cTnI in terms of formation,

surface characterization, affordability, and reproducibility (McClements et al., 2021). NanoMIPs have emerged as powerful tools in the biosensing field, and their integration into cTnI detection systems holds significant promise for enhancing sensitivity and selectivity in diagnostic assays. Through the imprinting process, these polymers can be tailored to recognize and bind specifically to cTnI, mimicking the binding characteristics of natural receptors while offering high stability and reproducibility. The synthesis process for imprinting is typically either one-pot bulk polymerization or surface imprinting onto a solid, with many more specific methods, such as substructure and dummy imprinting, commonly utilized (Mostafa et al., 2021; Ostrovidov et al., 2023). Conventionally, molecularly imprinted polymers (MIPs) are produced by self-assembly of specifically selected monomers and cross-linkers around the desired target, acting as a template (Vasapollo et al., 2011; Crapnell et al., 2020; Haupt et al., 2000). Whilst MIPs have high potential for use in diagnostic assays, they suffer from several drawbacks, namely heterogeneous binding affinity sites and slow binding kinetics. As such, nanoMIPs overcome these issues and enable optimal sensing performance (McClements et al., 2021). High-affinity nanoMIPs are produced via a similar approach where amino acid sequences derived from the target, cTnI, are immobilized onto functionalized glass beads, known as the solid-phase support. Subsequent polymerization of the functional monomers produces nanoMIPs around the immobilized target, with a two-step elution process ensuring only high-affinity nanoparticles are collected (Canfarotta et al., 2016).

In our prior research, high-affinity nanoMIPs were developed for sensing emerging cardiac biomarkers from spiked lab samples, specifically ST2, heart fatty acid-binding protein, and most recently cTnI (McClements et al., 2021; Crapnell et al., 2019). NanoMIPs were integrated with the heat-transfer method (HTM), an innovative thermal detection technique, creating a rapid and low-cost detection sensor platform coupled with straightforward analysis. In order to be suitable for medical diagnostics, nanoMIPs were functionalized onto low-cost and highly reproduceable screen-printed electrodes (SPEs) via electrografting and drop-casting. Previous works have incorporated thermocouples dip-coated with nanoMIPs; however, as ensuring a contamination-free environment is paramount for diagnostics, it is not cost-effective to dispose of each thermocouple after every use (Brinker, 2013). Additionally, our previous work required continuous sample introduction via an automated syringe pump, which demanded large sample volumes (2 mL) and further limited clinical feasibility (McClements et al., 2021). By redesigning the system for batch analysis, we reduced the required sample volume to just 30 µL, enabling the analysis of real clinical samples from patients. This refined methodology marks a significant departure from our previous work, creating a novel approach with the potential to improve MI treatment while reducing both diagnostic time and healthcare costs.

This study demonstrates that using thermal detection methods, and an optimized microfluidic device utilizing nanoMIP-functionalized SPEs can accurately measure cTnI concentrations in patient samples. We directly compare our results with well-established hospital protocols, a sandwich ELISA, and a CAPRI (Evaluating the effectiveness of intravenous Ciclosporin on reducing reperfusion injury in pAtients undergoing PRImary percutaneous coronary intervention) database containing patient variables such as body mass index (BMI), cTnT levels, and magnetic resonance image (MRI) values. We compare these values through statistical analysis to demonstrate that our results are statistically significant and clinically relevant to each patient. We also aim to explain our results regarding troponin complex release times, amino acid sequences (residuals) used for detection, and how the HTM differs from traditional absorbance-based immunoassays. Finally, a proof-of-concept study demonstrates the device's potential for measurements in patient plasma samples, further widening the number of viable blood matrices for this method.

Ultimately, our device can provide rapid and accurate blood cTnI levels at a significantly lower cost than the current gold standard

immunoassays. We also demonstrate a 50 % reduction in time to diagnosis (from 87 to 40 min) and sample volume (250–120 μL) compared to our previous work, both critical parameters to obtain effective MI diagnosis (McClements et al., 2021). Consequently, our results position this technology as a highly promising tool for MI diagnosis, thus creating the potential to improve patient outcomes and reduce healthcare costs.

2. Experimental

2.1. Equipment and reagents

4-aminobenzoic acid (4-ABA), 1,2-dichloroethane (EDC), hydrochloric acid (HCl), N-hydroxy succinimide (NHS), fetal bovine serum (FBS), phosphate buffered solution (PBS), and sodium nitrate were all purchased from Thermo Fischer Scientific (Loughborough, UK). Human serum albumin and plasma for blank samples, as well as ferricyanide, ferrocyanide, and potassium chloride (KCl) were purchased from Sigma Aldrich (Gillingham, UK). Deionized water (DI) was produced at Newcastle University with a resistivity of 18.2 M Ω cm. NanoMIPs were supplied by MIP Discovery and used a ~10 long amino acid sequence in the stable chain (AA:34-126) as the binding site (Canfarotta et al., 2016). Human serum and plasma patient samples were obtained from the CAPRI trial (www.clinicaltrials.gov NCT02390674, EudraCT number 2014-002628-29) at Newcastle-upon-Tyne Hospitals NHS Trust. The human samples used in this study had ethical approval obtained via IRAS project 149997. The trial was conducted in accordance with the principles of Good Clinical Practice and received a favorable ethical opinion from the National Research Ethics Committee North-East-—Newcastle and North Tyneside (14/NE/1070) on July 24, 2014 and a clinical trial authorization from the Medicines and Healthcare products Regulatory Agency on September 9, 2014.

SPEs were manufactured by Manchester Metropolitan University to the desired specifications. Briefly, the SPEs were fabricated in-house using a stencil design to achieve a 3.1 mm diameter working electrode using graphite ink (Product Ink: C2000802P2; Gwent Electronic Materials Ltd., Pontypool, United Kingdom) and were printed using a DEK 248 screen printer machine (DEK, Weymouth, UK) onto a polyester flexible film, 250 μm thickness (Autostat, Milan, Italy). The layer was cured in a fan oven at 60 $^{\circ}\text{C}$ for 30 min. Next, a silver/silver chloride reference electrode was introduced by screen-printing Ag/AgCl paste (Product Code: D2070423D5; Gwent Electronic Materials Ltd., Pontypool, UK) onto the polyester substrates and cured in a fan oven for 30 min at 60 °C. Finally, a dielectric paste (Product Code: D2070423D5; Gwent Electronic Materials Ltd., Pontypool, UK) was printed onto the polyester substrate to cover the connections and cured for an additional 30 min at 60 °C before use. This fabrication protocol ensures high repeatability and reliability, which has been robustly analyzed in terms of reproducibility in previous work by Roberto de Oliveira et al., confirming that there were no significant differences between electrodes (Roberto de Oliveira et al., 2023).

2.2. Screen-printed electrode functionalization

SPEs were functionalized with cTnI nanoMIPs via electrografting and drop-casting (McClements et al., 2021, 2022). A solution of 4-ABA (2 mm) and sodium nitrate (2 mm) in HCl (aqueous, 0.5 m) were mixed on an orbital shaker for 10 min; following this, a SPE was submerged within the solution, and cyclic voltammetry was conducted to attach 4-ABA to the substrate surface (Fig. S1). The electrode was rinsed with DI water to remove any unbound 4-ABA and then gently dried with nitrogen. To activate the carboxyl group, a solution of EDC (100 nm) and NHS (20 nm) in PBS buffer (pH = 5) was added to the surface of the SPE's working electrode via drop-casting (8 μ L). After 1 h, the SPE was rinsed with DI water and dried with nitrogen. Finally, a nanoMIP solution was gently vortexed, and 8 μ L was added to the SPE's working electrode surface to immobilize the nanoMIPs to the substrate via amide bonds. The

drop-cast solution was left for 8 h before it was rinsed with DI water and dried gently with nitrogen. The completed nanoMIP-functionalized SPEs were stored in PBS at 4 $^{\circ}$ C until their use.

2.3. Characterization of NanoMIPs

Atomic force microscopy (AFM) was performed using a Dimension Icon XR machine (Bruker, Nano GmbH, Berlin, Germany), where all imaging was carried out in air. Before imaging, nanoMIPs were dropcast onto Au-coated glass slides (Platypus Technologies, WI, USA) and left to dry at ambient conditions for 24 h. All image analysis was performed on Gwyddion 2.63, where mean values were calculated from measurements of 100 nanoMIPs. Dynamic light scattering (DLS) was conducted to measure the hydrodynamic diameter of the nanoMIPs using a Malvern Zetasizer Nano ZS (Malvern Instruments, Malvern, Worcestershire, UK). The instrument used a scattering angle of 173° and a laser wavelength of 632.8 nm, all experiments were performed at 25.0 \pm 0.1 °C.

2.4. Characterization of NanoMIP-Functionalized electrodes

Electrochemical impedance (EIS) measurements were performed on the PalmSens sensit smart potentiostat (PalmSens, Houten, The Netherlands). Measurements were taken at each stage of the immobilization protocol with a fixed frequency range of 0.1 Hz–100 kHz using PBS with ferricyanide (1 mM), ferrocyanide (1 mM), and KCl (0.1 M)

2.5. Sensing procedure

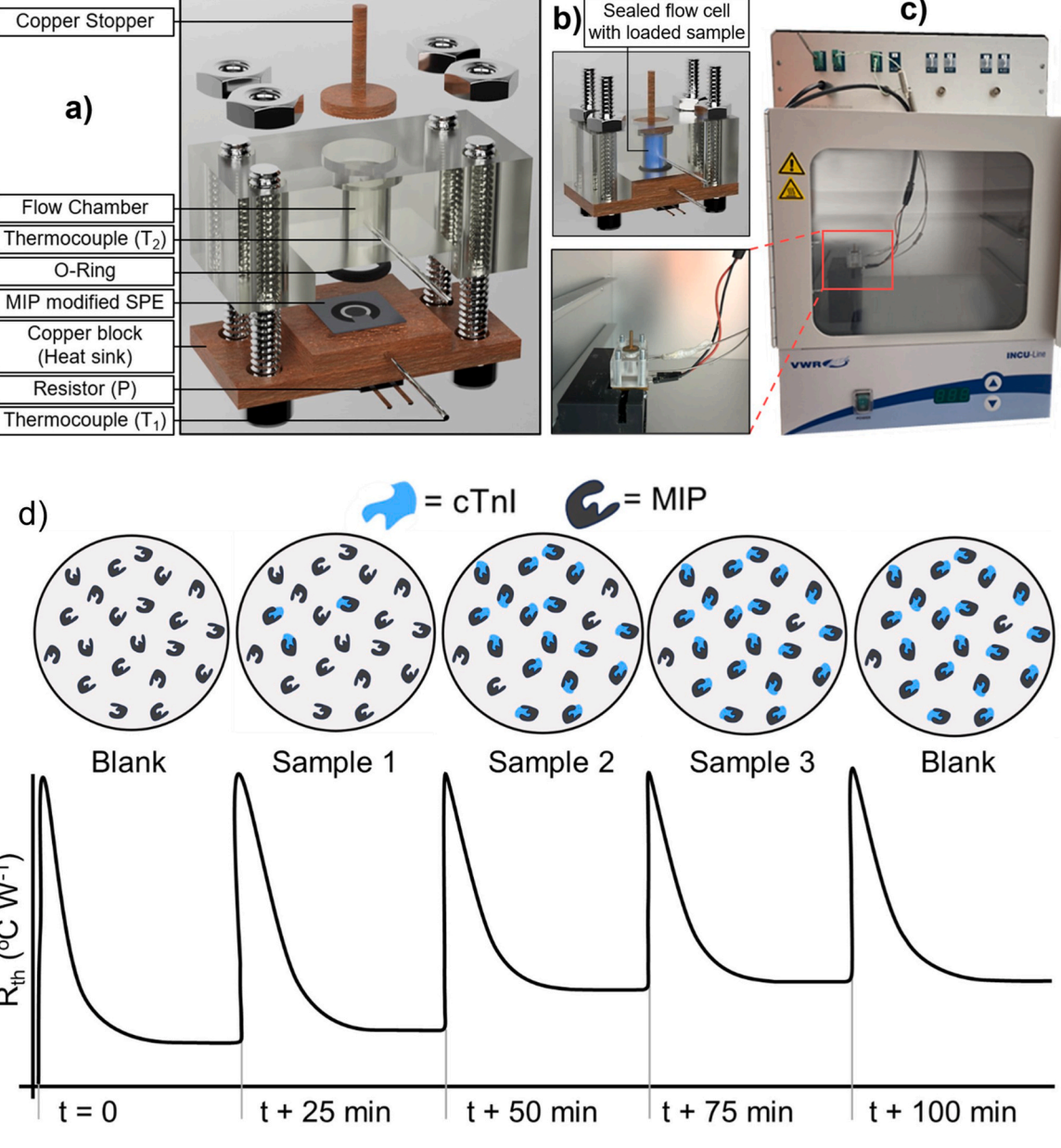
The microfluidic cell used for all thermal experiments is presented in Fig. 1a. A batch-modified version of the flow cell used by Crapnell et al. was produced in-house through 3D printing using an Anycubic Photon Mono with Anycubic Clear UV Resin (Shenzhen, China), forming the liquid chamber of the cell (Fig. 1b and S2) (Crapnell et al., 2019). For each run, the nanoMIP-functionalized SPE was placed at the center of the copper block with a rubber O-ring positioned on top of the SPE to avoid leakage, the resin cell was then added with four nuts and bolts tightened to ensure a good seal and placed within a controlled environment (Fig. 1c and S3).

Two type K thermocouples (RS Components, Corby, UK) were inserted into the measurement cell, T1 into the copper block heat sink and T₂ into the sample chamber (4 mm above the functionalized SPE). The measurement cell was then connected to the heat transfer device to allow temperature changes to be quantified, following the principles outlined by van Grinsven et al. (van Grinsven et al., 2010, 2014). In vivo conditions were mimicked through LabView software that actively controlled the temperature of the heat sink (T₁), set at 37.00 \pm 0.02 °C. This was controlled through an optimized proportional-integral-derivative controller (P = 1, I = 14, D = 0.3) connected to a power resistor (22 Ω) to ensure minimal feedback on the signal (Geerets et al., 2013). Temperature T₂ was measured each second, allowing the thermal resistance (Rth) to be determined, obtained through equation (1) (Canfarotta et al., 2018).

For all HTM measurements, three patient samples were examined per one functionalized SPE, meaning a typical experimental set consisted of a Blank – Sample 1 – Sample 2 – Sample 3 – Blank, with blank referring to human serum with no elevated cTnI levels (Fig. 1d). The first blank provides the R_{th} of the system and the final blank confirms that changes in R_{th} were due to cTnI binding rather than the characteristics of the human serum. For one sample, $120~\mu L$ of serum (or plasma) was added into the sample chamber, and a copper lid was added to reduce heat exchange with the external air. The system was left for 20 min to stabilize; once a plateau occurred, 100 data points were taken, and their average and standard deviation were recorded. Once the values had been taken the sample could be removed, and a new one added, with the process repeated.

Copper Stopper

C)



Sealed flow cell

Fig. 1. Experimental set-up for cTnI concentration measurements with a focus on the a) measurement cell design (Fig. S2 for cell dimensions), b) measurement cell under general operation, c) final lab HTM measurement setup with the measurement cell enclosed in a controlled environment (4250 × 2800 × 2600 mm, Fig. S3 for device dimensions) (van Grinsven et al., 2010, 2014), and d) the typical plot generated for one set of HTM measurements with cTnI binding.

3. Results and discussion

3.1. NanoMIP characterization

AFM measurements revealed that drop-cast nanoMIPs (0.621 mg mL⁻¹) form a densely packed layer with high surface coverage (Fig. S1). They had spherical morphologies and a mean diameter of 78 \pm 12 nm, demonstrating their homogeneous size distribution and validates the synthesis process (Fig. S1). DLS analysis revealed a mean diameter of 89 nm, slightly larger than the AFM measurements. This variation can be attributed to the differing states in which the nanoMIPs were analyzed. Specifically, DLS was conducted in DI water, whereas the AFM measurements were taken in a dry state, indicating that the nanoMIPs experienced minimal swelling.

3.2. Quantification of bound cTnI to NanoMIPs

The amount of bindable cTnI present within a sample can be quantified through the change in thermal resistance (ΔR_{th} , Fig. 1d). When more cTnI binds to the nanoMIPs it causes a greater insulating effect, decreasing the temperature of the liquid sample, leading to a greater ΔR_{th} . Resistance values were obtained using equation (1):

$$R_{th} = \frac{T_1 - T_2}{P} \tag{1}$$

where, T_1 was the heat sink temperature, maintained at 37.00 \pm 0.20 $^{\circ}\text{C}$ through variation of the power supplied (P), and T₂ was the temperature of the liquid in the sample chamber (Canfarotta et al., 2018). Firstly, the effectiveness of the nanoMIP-functionalized SPE was confirmed through baseline responses utilizing cTnI-spiked buffer solutions (Fig. S4). The results confirmed that the observed ΔR_{th} was significant enough to allow for the sensing of cTnI within the desired concentration range.

Additionally, the feasibility of running three patient samples per SPE was assessed. It was shown that the results obtained were comparable to running one sample per SPE, suggesting no significant impact and that multiple samples can be used per SPE, reducing waste (Fig. S5). Theoretically, more samples could be measured per SPE due to the highest spiked concentration of cTnI trialed being much greater than those in MI patients (1000 vs. 1–150 ng $\rm L^{-1}$). However, three samples per SPE was selected to avoid any SPE saturation; additionally, within a clinical setting, reusing more than this could potentially introduce cross-contamination.

An example of a theoretical R_{th} vs. time plot is presented in Fig. 1d, with the corresponding amount of cTnI occupying nanoMIP binding sites shown. This process was conducted on nine sets of patient samples with confirmed acute MI, with each set containing blood from six sample times: pre-serum (t = 0 min, post reperfusion), t = 5 min, t = 15 min, t = 30 min, t = 90 min, and t = 24–48 h. A typical set of R_{th} results is presented for Patient 6 (Fig. 2a). Upon each sample addition, further binding occurs, increasing the R_{th} of the surface. For Patient 6, the greatest R_{th} increase occurred at the 90 min sample ($\Delta R_{th} = 0.622~^{\circ}C$ W $^{-1}$), suggesting that this sample point corresponds to the highest degree of cTnI binding. A sample with a large ΔR_{th} indicates a high cTnI concentration as more has bound to the nanoMIPs on the SPE, thus increasing the R_{th} .

3.3. Patient cTnI concentrations

To convert ΔR_{th} values to cTnI concentration, calibration standards were produced using human serum albumin and examined via thermal analysis at clinically relevant cTnI concentrations (0.1, 1, 10, 100, 1000 ng L^{-1} , Fig. S6). An exponential relationship was observed between the

two axes, exhibiting an excellent fit with an appropriate R^2 value of 0.957, showing conversion of ΔR_{th} to concentration can be conducted with a high degree of certainty (Fig. 2b). A similar procedure was followed for conversion from ELISA absorbance values to cTnI concentration (Fig. S7), which also resulted in an excellent exponential fit between the two variables ($R^2=0.953$). cTnI concentrations from our HTM nanoMIP method could then be compared to results from an ELISA immunoassay and the CAPRI database.

After device calibration, patient samples were examined, where variation in cTnI concentration at each sample time can be associated with multiple factors. This included sample location, the anatomical site where the blood sample was extracted, time since onset of symptoms, and numerous discrete variables, such as the type of drug administered and patient lifestyle. Generally, an increase in cTnI indicates greater damage to the cardiac tissue (Park et al., 2017). Patient cTnI concentration values obtained through thermal analysis demonstrated a peak in cTnI at 15 or 90 min (Fig. 2b and c), indicating the greatest amount of bindable cTnI. Regardless of peak cTnI time, the percentage increase from the baseline value (pre, t = 0) to the peak value was significant. Indicated by an increase in cTnI levels of >1000 % from their baseline, except for Patient 5 (Fig. 2d). Furthermore, all patient samples had very little cTnI present in the 24–48 h sample, which is somewhat surprising as cTnI levels within the blood should not drop this quickly following MI. These results can be further understood through comparison against the CAPRI database (Section 2.4) and results obtained from an ELISA (Section 2.5).

3.4. Statistical significance with CAPRI

After cTnI results were obtained from thermal measurements, a

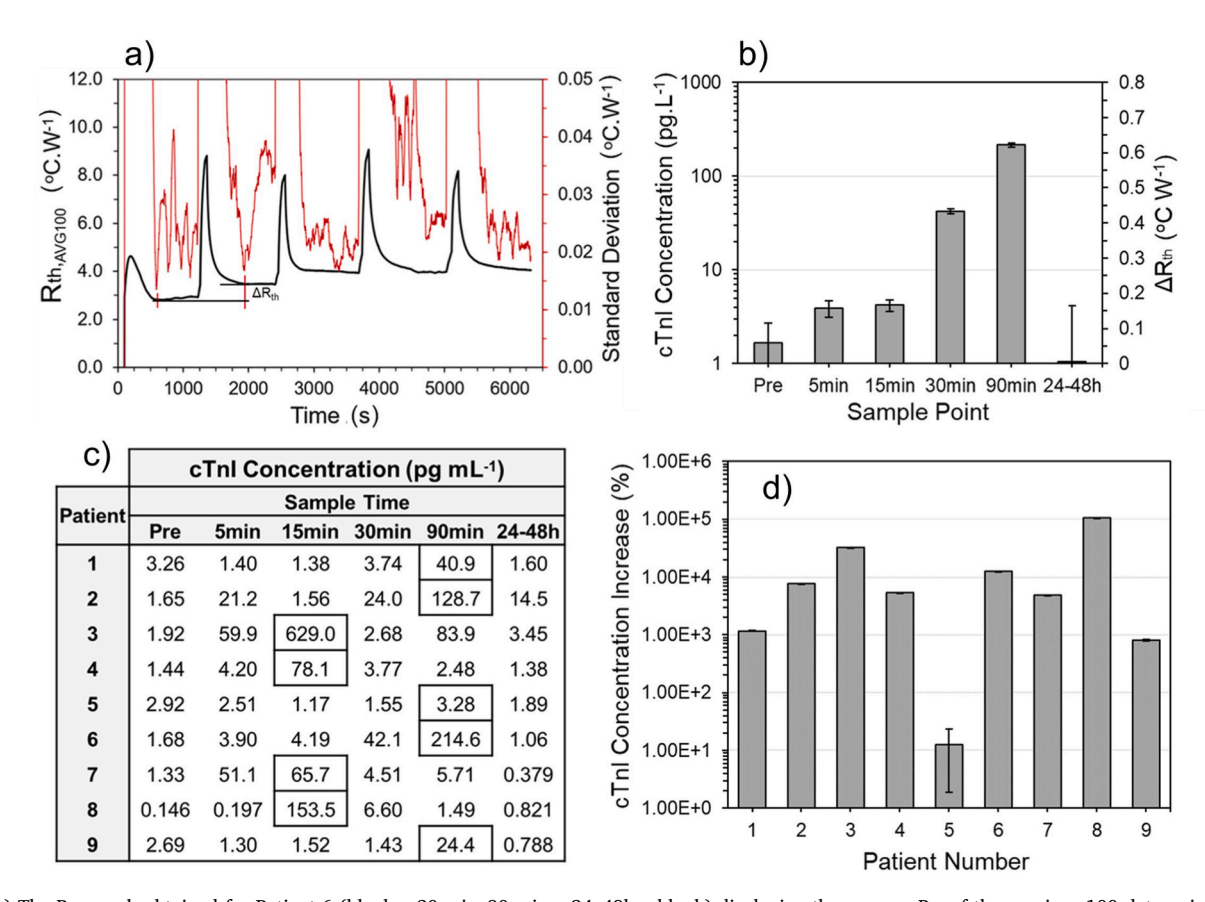


Fig. 2. a) The R_{th} graph obtained for Patient 6 (blank – 30 min–90 min – 24–48h – blank) displaying the average R_{th} of the previous 100 data points and corresponding standard deviation. b) cTnI concentration for Patient 6 at each sample time with the corresponding ΔR_{th} values. c) Table of cTnI concentrations for each patient at each sample time with the peak concentration identified by a black box. d) Plot showing the percentage increase from the baseline (pre) cTnI concentration to the peak concentration value for each patient.

comparison was made against a database of patient variables. Values obtained from the CAPRI trial were used as they accounted for all patients investigated in our work (Cormack et al., 2020). The trial was a randomized, double-blinded, controlled study conducted at a single center, comparing Ciclosporin to placebo (saline) in patients confirmed to have suffered a MI. For this statistical analysis, cTnT concentration and values obtained from MRI scans, such as the left ventricular ejection fraction and infarction size were utilized. Both cTnT measurements and

MRI scans are frequently used in hospitals as indicators for MI and as such are a reliable benchmark for comparison with our study's cTnI results. The changes in these database values and results within this study were investigated in terms of absolute and percent change, as well as expressed over linear and logarithmic scales. In some instances, it was required for the logarithmic trend to be observed due to the exponential relationship present when converting from ΔR_{th} to cTnI concentration (Fig. S6).

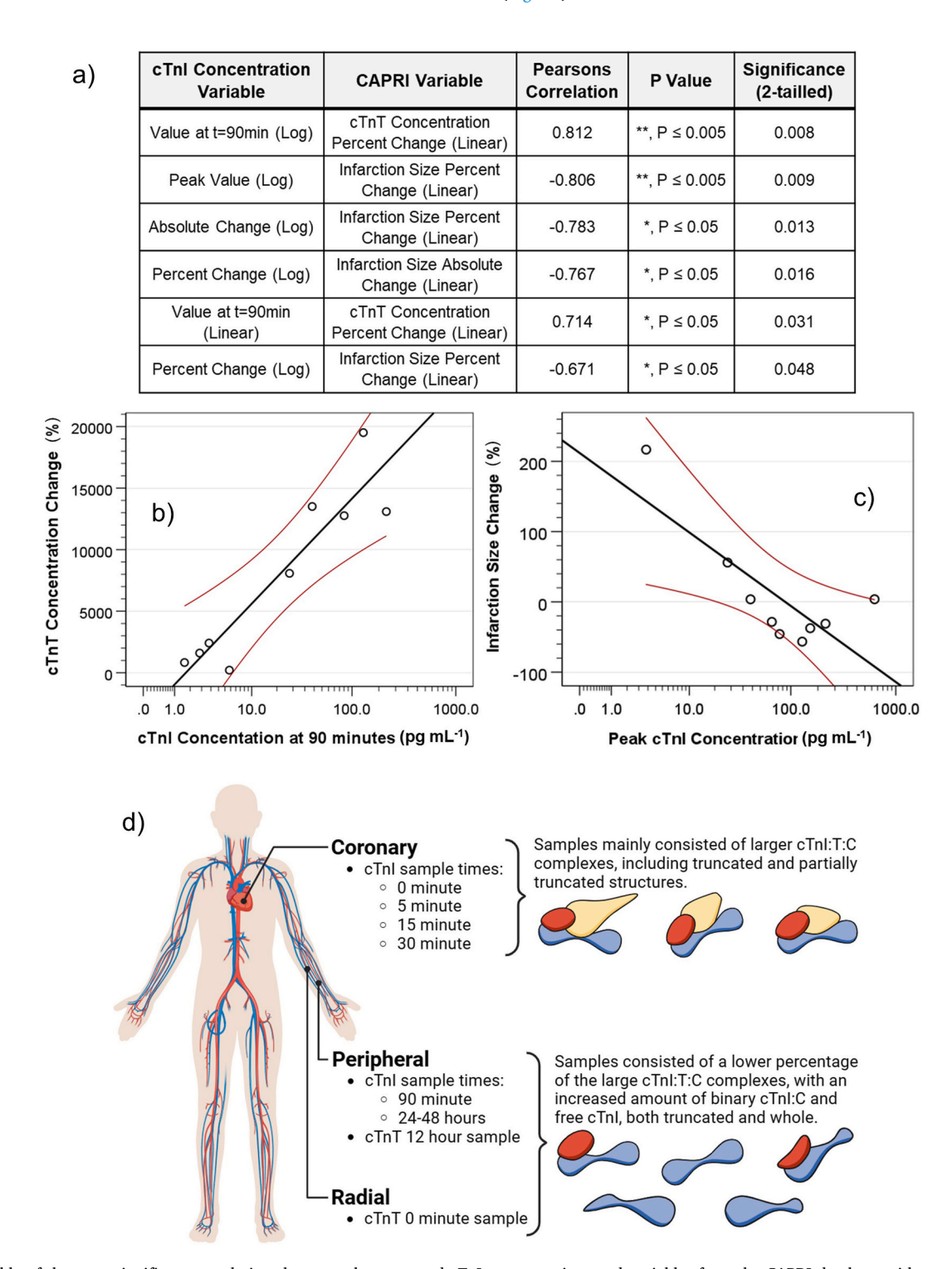


Fig. 3. a) Table of the most significant correlations between the measured cTnI concentrations and variables from the CAPRI database with examples of b) the strongest correlation observed: cTnT concentration change indicates the increase observed between the blood samples taken at t=0 and t=12 h, and c) the second strongest correlation: infarction size change relates to the measured change in bloods taken at t=0 and $t=82\pm4$ days (both plots include 95 % confidence intervals and their associated R^2 values). d) Schematic identifying blood sample locations and the cTnI composition associated with each.

Statistical analysis was conducted using the Pearson bivariate correlation to indicate correlation strength and the significance of the obtained relation (IBM's SPSS software) (Corp., 2024). The six strongest correlations can be observed in Fig. 3a, with b) and c) illustrating this for the two most correlated results, cTnI concentration at 90 min vs. cTnT concentration change and peak cTnI concentration vs. infarction size change. Blood samples for these variables were taken from one of three locations: the coronary artery, peripheral vein, or radial artery (Fig. 3d) (Cormack et al., 2020; Damen et al., 2020). A strong correlation existed between the change in cTnT concentration (%) between the baseline value (t = 0) and the 12 h sample, indicative of the amount of damage sustained to the heart muscle, with our cTnI concentration at 90 min (Fig. 3b) (Korff et al., 2006; Potter et al., 2022). The 90 min cTnI sample is the first taken from the periphery and, therefore, can be more easily compared to the cTnT bloods also taken from exterior blood vessels. A larger 90 min cTnI concentration coincides with a larger increase in cTnT, suggesting that the results produced by the HTM nanoMIP methodology are comparable to the size of the MI.

It is difficult to compare cTnI values obtained from the coronary region with CAPRI variables obtained from the periphery/radial due to the variation in types of cTnI complex and the presence of additional particles in the coronary blood (Damen et al., 2020). Consequently, additional methods for MI size quantification, such as MRI scans, can be employed. One such parameter is the infarct size, which relates to the amount of heart tissue death or necrosis present (Saleh et al., 2018). Another good correlation is exhibited between infarction size change (%) from the baseline (t = 0) to the 3-month post-MI scan and peak cTnI value Fig. 3c). The patients with larger cTnI concentrations experience a greater reduction in infarction size. This is expected as a higher amount of cTnI released into the blood stream indicates more damage to the heart muscle, and a greater decrease in infarct size would suggest that more heart tissue has been repaired following a more severe MI. Notably, our findings demonstrate robust correlations between cTnI levels and variables within the CAPRI database, emphasizing the potential of thermal detection via nanoMIPs in assessing the extent of heart muscle damage.

3.5. Comparison with ELISA

A direct comparison of cTnI levels of the patient samples was performed between the HTM and a current "gold standard" sandwich cTnI ELISA immunoassay (antibodies.com, A77930) (Hornbeck, 2015). The ELISA measurements were conducted on all sample times for five of the nine patients (Patients 1, 2, 4, 8, 9), allowing three repeats per sample and a set of standards to fit onto one 96-well plate ELISA. At each sample time the cTnI concentration differs, depending on which quantification method is employed. For Patient 9, it is clear that there is minimal cTnI recorded for the HTM 24-48 h sample and that the cTnI peak occurs at different sample times (Fig. 4a). However, when the 24-48 h sample is excluded, all remaining cTnI values demonstrate agreeable results in terms of magnitude. Upon comparison of the remaining patients (Fig. S8), peak cTnI concentration occurred in the 15 or 90 min samples for the HTM, and the 90 min or 24-48 h samples for the ELISAs. Our novel nanoMIP-HTM platform demonstrates excellent reproducibility in clinically relevant cTnI concentration ranges. Crucially, when cTnI levels are elevated, such as at the 90-min sample point (Fig. 4a), the system achieved a coefficient of variance of 8.2 %, aligning with established ELISA of 6.0 %, both below the 10.0 % threshold. While higher coefficient of variance values were observed for earlier time points (e.g., 5 min, 15 min), this is expected in undiluted clinical samples where biomarker concentrations are low and prone to biological variability. Importantly, despite these early fluctuations, key trends in cTnI concentration remained consistent across replicates, reinforcing the robustness of our platform for diagnostic applications. We found only a limited number of studies that employed clinical samples for cTnI detection, with many relying on spiked samples (e.g., PBS or human serum/plasma). Notably, some studies such as those by Wang et al. (2023), Zhan et al., 2022, and others utilized diluted samples (5–10x), which complicates direct comparison with our method (Wang et al., 2023; Zhan et al., 2022b). Diluting clinical samples reduces the concentrations of interfering molecules, which can improve signal clarity

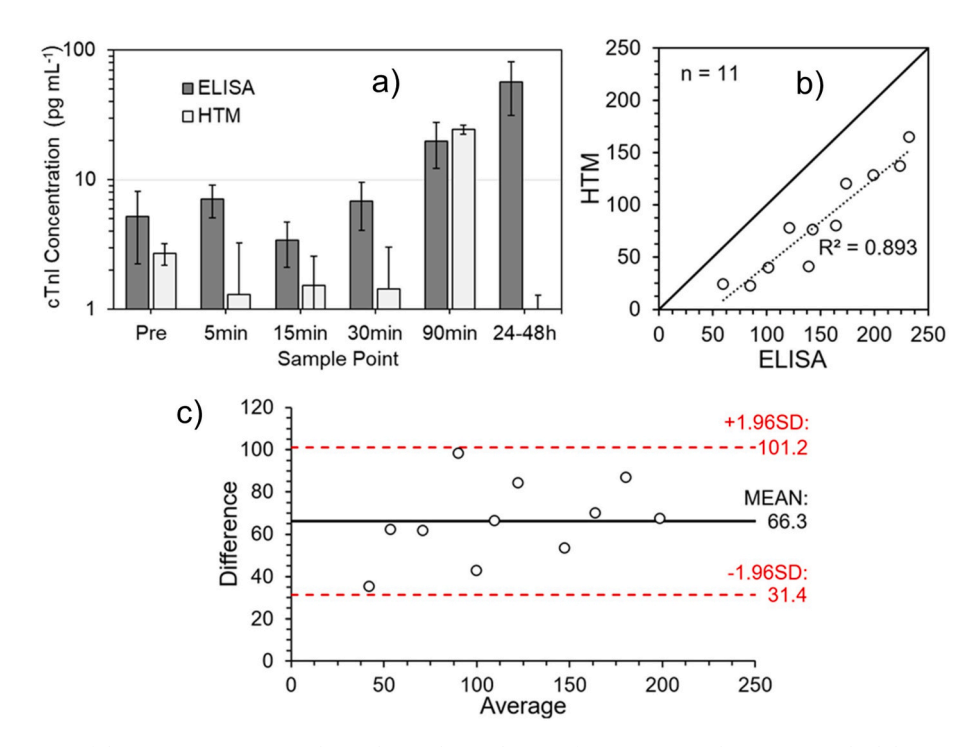


Fig. 4. a) A typical comparison of the cTnI concentrations obtained at each sample point for Patient 9, with average standard deviations of 3.53 and 1.27 for the ELISA and HTM methods, respectively (A linear plot can be found in Fig. S8), and all patient results are presented in Fig. S9). b) Regression line for the peak cTnI values between the "gold standard" ELISA method and the HTM. c) A Bland-Altman plot to analyze the agreement between the two different assays, where a bias of +66.3 can be observed.

but compromises the accuracy and real-world applicability of the test. This limitation is particularly relevant for point-of-care (PoC) settings, where sample integrity is crucial. In contrast, our method employs undiluted clinical samples, preserving the native biomarker environment and ensuring reliable results that better reflect true physiological conditions.

Fig. 4b and c relate the peak cTnI concentrations observed in terms of simple regression and Bland-Altman plots, respectively, to understand the relatability between the two methods. Fig. 4b shows a strong correlation between the HTM and ELISA, suggesting the HTM methodology can indicate which patients have the highest cTnI levels. However, an offset between the two methods exists, with the linear trend deviating from the x = y reference line and the Bland-Altman plot showing a +66.3 bias. The discrepancy between the HTM and ELISA results can be attributed to varying binding epitopes, interfering factors, and troponin complex release times. A single amino acid difference within an epitope can significantly impact target binding, and therefore, interpreting data produced by immunoassays with different epitopes is challenging (Guy et al., 2013). Specifically, the epitopes used for binding sites in the HTM and ELISA methods may differ, leading to variations in binding site availability within different complexes. The ~10 amino acid sequence used to form the cTnI-nanoMIP binding is located within the stable chain (AA:34-126) and is the only section used for binding. In contrast, commonly available immunoassays often employ up to four binding sites, potentially explaining the bias observed in Fig. 4c, as the nanoMIPs rely on only one binding site. As such, reduction in site availability due to interfering factors with non-specific adsorption of interfering molecules, epitope blocking by autoantibodies, or interaction of the cTnI with cardiotonic drugs would be more impactful to the HTM than the ELISA (Eriksson et al., 2005; Regan et al., 2019; Lippi et al., 2012). Therefore, a correction factor may be introduced to account for the reduced cTnI concentration provided by the HTM.

Additional differences between the HTM and ELISA results can be attributed to changes in troponin complex size and structure, and complex release time and volume (Lippi et al., 2012; Denessen et al., 2023; Morjana, 1998). These factors may explain the observed spike in cTnI concentrations at 15 and 90 min for the HTM. Following MI onset, cTnI begins to appear in the blood within 3-6 h and peaks after 12-24 h, with cTnI being released as a monophasic single peak (Park et al., 2017; Lippi et al., 2012; Katrukha et al., 2020; Collinson et al., 2001; Giannitsis et al., 2013). After this, free cTnI is soon detected before any troponin complex forms, such as the ternary cTnI:T:C and the more common binary cTnI:C (Park et al., 2017; Gaze et al., 2008; Lippi et al., 2012; Denessen et al., 2023). In addition to release, the degradation of troponin complexes and free cTnI also impacts the types of cTnI observed through our method (Fig. 5a). Firstly, cTnI:T:C complexes can degrade into lower molecular weight forms over time via the truncation of the long amino acid chains of the cTnI and cTnT, as well as separating down into its three individual proteins (Denessen et al., 2023; Vylegzhanina et al., 2019). Additionally, the free form of cTnI is susceptible to degradation, especially via proteolytic enzymes (Denessen et al., 2023; Morjana, 1998). This enzymatic cleavage occurs in the amino acid sequence on either side of the stable cTnI region (AA:34-126) in the N-terminal (amino acids <34) or C-terminal (amino acids >126), where protection provided by the binding of the cTnI with cTnT and/or cTnC is absent (Lippi et al., 2012; Katrukha et al., 2020; Krudy et al., 1994). This stable region is where most binding epitopes in immunoassays are located, including the one within this study, allowing for many different-sized troponin molecules to bind (Park et al., 2017). It has been demonstrated that this truncation can occur within the first 90 min of MI onset and can result in up to 11 different cTnI fragment lengths all containing the stable region required for binding (12-23 kDa) (Gaze et al., 2008; Denessen et al., 2023; Morjana, 1998; Madsen et al., 2006). In some instances, these shortened cTnI structures can interact with other truncated cTnT and cTnC complexes through transglutamination to form new structures of various molecular weights (Lippi et al., 2012).

Variations in troponin complex morphology and differing binding site, make direct comparisons between detection methods challenging. For our HTM-based detection method, the degree of thermal insulation provided to the functionalized surface may vary with complex size, be it full length or a proteolytic fragment (Katrukha et al., 2020). In the early peaks at 15 and 90 min, we may detect the release of a small number of large complexes that provide more thermal resistance than smaller molecules that go undetected in absorbance-based methods (Fig. 5b). This is especially true when considering the impact distance from the troponin release site has on degradation. Damen et al. identified a higher concentration of larger complexes, such as cTnI:T:C, in the coronary veins compared to peripheral circulation (Damen et al., 2020; Denessen et al., 2023). This is significant as the samples within this study were taken from various locations depending on sample time, with t = 0, 5, 15, and 30 min taken directly from the coronary and the 90 min and 24-48 h samples taken from peripheral blood. Future work will explore imprinting of nanoMIPs with binding sites of varying lengths of amino acids and incorporating multiple binding locations. This approach aims to enhance sensitivity and specificity, allowing for a more effective comparison with existing ELISAs.

3.6. Measurements in plasma

Within hospitals, it is common for both blood serum and plasma samples to be used for various tests; therefore, a proof-of-concept device that performed cTnI measurements in plasma was trialed. Plasma and serum contain similar proteins and electrolytes; however, anticoagulants (e.g., ethylenediaminetetraacetic acid (EDTA), heparin, and citrate) are typically added to plasma samples to prevent clotting (Vignoli et al., 2022). Therefore, Fig. 6 demonstrates how anticoagulants may alter the ΔR_{th} obtained from HTM measurements (Erickson, 2009; Hall et al., 1959; Mair et al., 1994). Each patient's plasma sample had a lower peak ΔR_{th} than the corresponding serum sample, but the peak values still occurred at 90 min.

It is well documented that differing concentrations of cardiac troponins can be obtained from serum and plasma samples from the same patient. Moreover, the anticoagulant used can alter levels, with Vignoli et al. demonstrating that several metabolites showed statistically significant alterations among different matrices, potentially impacting clinical judgment (Kavsak et al., 2018; Herman et al., 2017). For example, in our work, EDTA can break up troponin complexes into its three subunits, which would result in a smaller R_{th} due to only the free cTnI binding to the nanoMIPs rather than the larger ternary complex (Vylegzhanina et al., 2019; Kavsak et al., 2020; Wu et al., 1998). This and the fact that interfering factors will interact differently depending on the binding epitope used results in the reduced ΔR_{th} . However, Fig. 6 does show that the MIP–based sensors using HTM as read–out can accurately detect cTnI in plasma, with Patient 1 having a lower ΔR_{th} than Patient 2 for both the plasma and serum samples.

3.7. Applicability for point-of-care detection

Predominantly, cTnI detection occurs in laboratories, yet there is an urgent need to expedite clinical diagnosis for acute MI. PoC testing presents a viable solution, a diagnostic approach that operates without requiring elaborate infrastructure or complex instruments. Introducing compact benchtop instruments and handheld devices to enable bedside cTnI testing will significantly reduce time to diagnosis, significantly improving patient outcome (Chen et al., 2023). Although our current device is not yet a finalized PoC platform, the principles employed, and its compact size provide a strong foundation for translation to a bedside device. The methodology outlined in this study holds promise in addressing several common limitations of PoC biomarker detection devices. Namely, current PoC devices lack accuracy and precision when compared to high-sensitivity cTnI assays conducted in laboratory settings (Campu et al., 2022). Additionally, state-of-the-art ELISAs

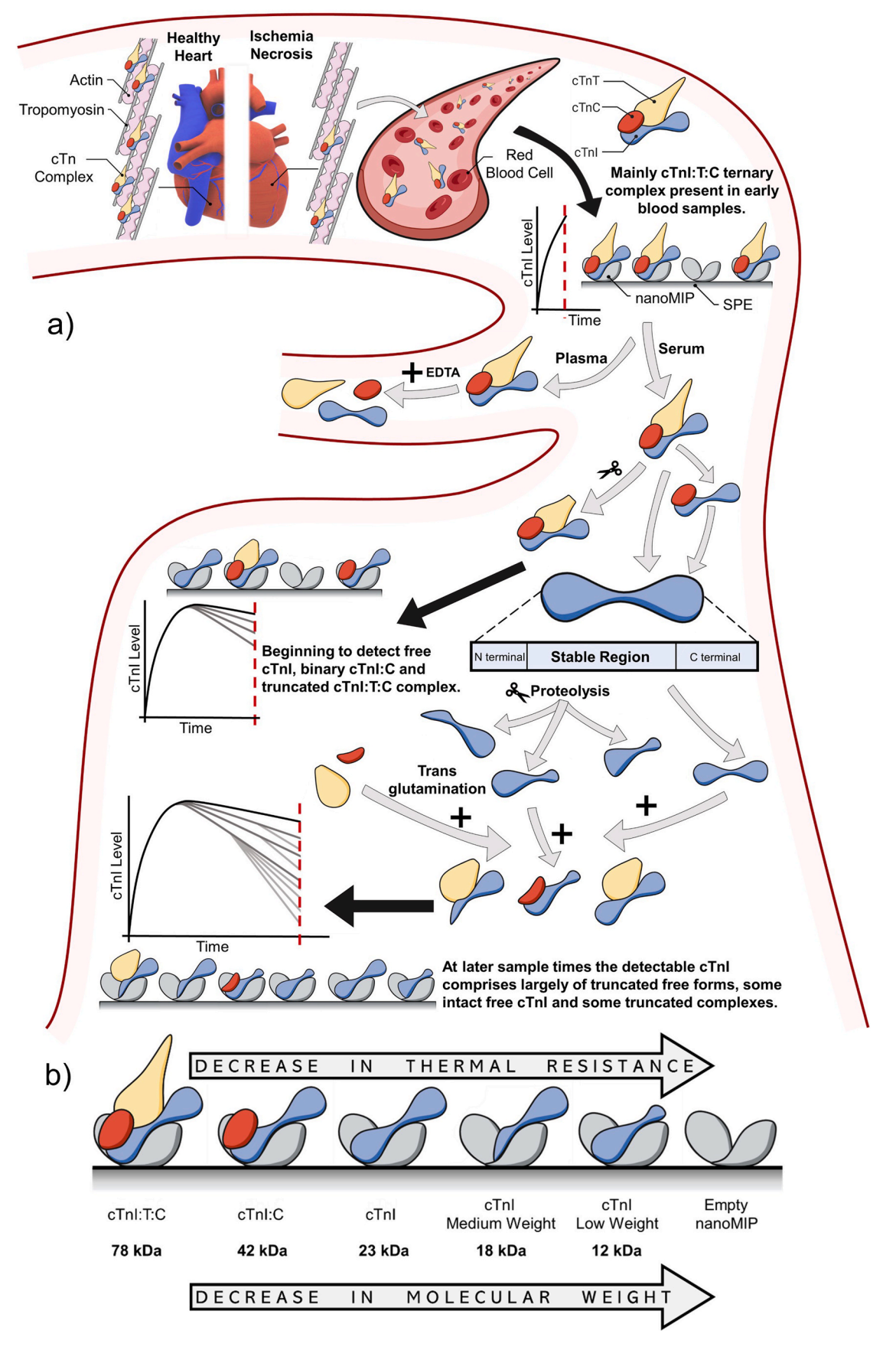


Fig. 5. a) Schematic showing the lifecycle of troponin following a MI, indicating the types of complexes present at various sample times, as well as the degradation and truncation that occurs within the amino acid sequences of each protein and b) a schematic highlighting how cTnI complex size can impact R_{th} , from the most thermally insulating, cTnI:T:C ternary complex, to the least, an unoccupied nanoMIP.

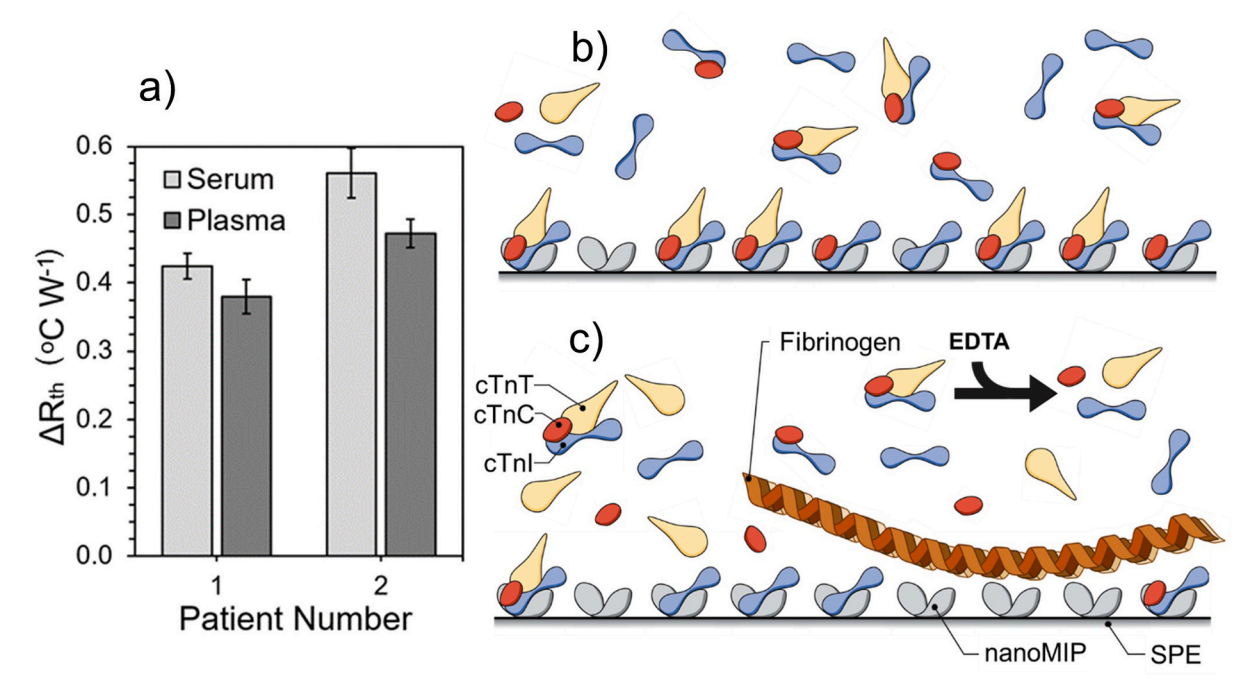


Fig. 6. a) Comparison of peak ΔR_{th} values for blood plasma and serum samples for two patients (sample time = 90 min), and a schematic to show the difference between interactions of cTnI with the nanoMIP in b) serum and c) plasma (fibrinogen to scale with the troponin molecules).

typically necessitate the use of large UV–Vis spectrophotometers, making this analysis technique incompatible for transition to a portable or bedside device. Finally, many novel cTnI sensing methods with promising results face challenges in terms of scalability and the development of multiplexing (Campu et al., 2022).

ELISAs suffer from several drawbacks, including labor and cost, due to the procedure's complexity, reliance on expensive culture cell media for specific antibodies, and antibody instability requiring refrigerated transport and storage (limiting shelf life) (Sakamoto et al., 2018). Furthermore, antibody and aptamer-based detection systems are prone to false results due to the cross-reactivity of some molecules with the detection site (Sakamoto et al., 2018; Dhara et al., 2020). Novel measurement methods also face challenges and drawbacks in their implementation as PoC cTnI detection devices. For instance, surface plasmon resonance and fluorescence measurements may lack the sensitivity necessary for clinical diagnosis, with the former also being very expensive and complicated and the latter heavily reliant on light stability (Chen et al., 2023; Campu et al., 2022). Additionally, interference from background signals, leading to result variability, is another significant problem; this is particularly evident in surface-enhanced Raman scattering and electrochemical approaches. For each instance, modification of these approaches into multiplex devices remains unattainable (Chen et al., 2023; Campu et al., 2022).

These challenges can be overcome by utilizing nanoMIPs coupled with thermal analysis. Compared to biological entities, nanoMIPs offer numerous advantages, including vastly superior stability, simple preparation, high selectivity and affinity, long-term storage without freezing, and cost-effectiveness, rendering them attractive for analytical applications (Sarvutiene et al., 2024). Choudhary and Altintas successfully developed a biomimetic sensor using high-affinity nanoMIPs, achieving a LoD below the threshold required for clinical environments. However, the use of gold chips increases the cost per test, making it less cost-efficient, and the complex sample preparation required prior to analysis reduces its practicality in time-sensitive settings (Choudhary et al., 2023). Additionally, despite extensive testing on spiked PBS samples, the study lacks evidence of the sensor's efficacy in real or artificial samples, which could affect both its clinical relevance and compatibility with the portable SPR's microfluidics due to differences in

sample density and viscosity (Choudhary et al., 2023). Moreover, integrating thermal analysis for cTnI quantification employs a straightforward protocol that necessitates relatively few components, enabling the development of a compact device and a simplified operating procedure that requires minimal training. Additionally, since the system proposed in this study operates under batch operation, it is feasible for multiple cells to function in parallel, facilitating easy multiplexing of this methodology. Moreover, with the existing lab device measuring 4250 \times 2800 \times 2600 mm (Fig. 1a–c and S3), it could already be incorporated into a portable, trolley-based device for use on a ward. Meanwhile, further work is underway to develop a fully portable version that can be carried by paramedics. The proposed device in this body of work not only offers a next generation sensing tool that will elevate clinical treatment but also allow developing countries the same diagnosis standards due to the economically viable nature of nanoMIP based detection systems.

4. Conclusion

The study introduces a cardiac troponin biosensor using nanoMIPs to detect cTnI concentrations in post MI patient samples, featuring a rapid (40 min) and low-volume (120 µL) methodology with thermal resistance indicating cTnI concentrations accurately. It offers environmental stability, simplicity, selectivity, and cost-effectiveness, surpassing current cTnI sensing methods. Detection via thermal analysis shows comparable performance to a high-sensitivity ELISA, identifying patients with high cTnI levels accurately, albeit with a systematic bias requiring correction factors. The methodology's early peaks in cTnI concentration are attributed to serum complexity, and difficulties in comparing detection methods that utilize different epitomes. Correlations with clinical parameters validate the results, emphasizing its potential for MI diagnosis enhancement. With strong correlations observed between our measured cTnI values and key clinical parameters: cTnT levels and infarction size. The correlation between variables known to indicate the size of MI and our results further supports the validity of the obtained results.

This study emphasizes the applicability for nanoMIPs sensors for use in sensitive cTnI detection from patient blood serum samples. Further refinements should explore the impact troponin complex size variation has on detection, not only within our thermal methodology but also in

well-established methods. Little comment has been made on this in literature, and consideration should be taken into how degradation of the target molecule may alter observed levels. However, this methodology holds the prospect of enhancing diagnostic capabilities in cardiovascular medicine, potentially contributing to more personalized and effective patient care. As a result, our findings indicate that this technology holds great promise as a valuable tool for PoC diagnosis of MI, potentially leading to decreased healthcare expenses and enhanced patient outcomes.

CRediT authorship contribution statement

Joshua Saczek: Writing - original draft, Visualization, Validation, Methodology, Investigation, Formal analysis, Conceptualization. Oliver Jamieson: Writing - review & editing, Visualization, Validation, Methodology, Investigation, Conceptualization. Jake McClements: Writing - review & editing, Visualization, Supervision, Methodology. Amy Dann: Writing - review & editing, Visualization, Investigation. Rhiannon E. Johnson: Investigation. Alexander D. Stokes: Investigation. Robert D. Crapnell: Writing - review & editing, Resources. Craig E. Banks: Writing - review & editing, Resources. Francesco Canfarotta: Writing - review & editing, Resources. Ioakim Spyridopoulos: Writing - review & editing, Resources. Alan Thomson: Writing - review & editing, Resources. Azfar Zaman: Writing - review & editing, Funding acquisition. Katarina Novakovic: Writing - review & editing, Supervision, Funding acquisition. Marloes Peeters: Writing review & editing, Supervision, Resources, Project administration, Methodology, Funding acquisition, Conceptualization.

Declaration of competing interest

The authors declare that they have no known competing financial interests or personal relationships that could have appeared to influence the work reported in this paper. Specifically, while nanoMIPs were supplied by MIP Discovery for research purposes, there are no financial or other relationships with the company that could affect the outcomes of this study.

Declaration of competing interest

The authors have no declaration of interest to declare.

Acknowledgments

MP, JMC, KN, and IS would like to acknowledge funding from the Rosetrees Trust [Seedcorn2020_100303] for undertaking this work OJ would like to thank the MRC Confidence in Concept for salary, whereas support for salary of AD is provided via the USDA National Institute of Food and Agriculture, [AFRI project NIFA 2022-67021-36408]. An EPSRC Impact Accelerator Account has provided support for funding of JS and AS, in addition to providing support for consumables.

Appendix A. Supplementary data

Supplementary data to this article can be found online at https://doi.org/10.1016/j.bios.2025.117467.

Data availability

Data will be made available on request.

References

Barrett-Connor, E., Khaw, K.-T., 1984. Family history of heart attack as an independent predictor of death due to cardiovascular disease. Circulation 69, 1065–1069.
 Benjamin, E.J., Blaha, M.J., Chiuve, S.E., Cushman, M., Das, S.R., Deo, R., De Ferranti, S. D., Floyd, J., Fornage, M., Gillespie, C., 2017. Heart disease and stroke

- statistics—2017 update: a report from the American heart association. Circulation 135, e146–e603.
- Boersma, E., Maas, A.C., Deckers, J.W., Simoons, M.L., 1996. Early thrombolytic treatment in acute myocardial infarction: reappraisal of the golden hour. Lancet 348, 771–775
- Brinker, C., 2013. Dip coating. Chemical Solution Deposition of Functional Oxide Thin Films. Springer, Vienna, Austria.
- Campu, A., Muresan, I., Craciun, A.M., Cainap, S., Astilean, S., Focsan, M., 2022. Cardiac troponin biosensor designs: current developments and remaining challenges. Int. J. Mol. Sci. 23. https://doi.org/10.3390/ijms23147728.
- Canfarotta, F., Poma, A., Guerreiro, A., Piletsky, S., 2016. Solid-phase synthesis of molecularly imprinted nanoparticles. Nat. Protoc. 11, 443–455. https://doi.org/ 10.1038/nprot.2016.030.
- Canfarotta, F., Czulak, J., Betlem, K., Sachdeva, A., Eersels, K., van Grinsven, B., Cleij, T. J., Peeters, M., 2018. A novel thermal detection method based on molecularly imprinted nanoparticles as recognition elements. Nanoscale 10, 2081–2089. https://doi.org/10.1039/C7NR07785H.
- Capewell, S., McMurray, J., 2000. "chest pain—please admit": is there an alternative? A rapid cardiological assessment service may prevent unnecessary admissions 320, 951–952. https://doi.org/10.1136/bmj.320.7240.951.
- Chen, Q., Wu, W., Wang, K., Han, Z., Yang, C., 2023. Methods for detecting of cardiac troponin I biomarkers for myocardial infarction using biosensors: a narrative review of recent research. J. Thorac. Dis. 15, 5112–5121. https://doi.org/10.21037/jtd-23-1263.
- Choudhary, S., Altintas, Z., 2023. Development of a point-of-care SPR sensor for the diagnosis of acute myocardial infarction. Biosensors 13, 229.
- Collinson, P.O., Boa, F.G., Gaze, D.C., 2001. Measurement of cardiac troponins. Ann. Clin. Biochem. 38, 423–449.
- Cormack, S., Mohammed, A., Panahi, P., Das, R., Steel, A.J., Chadwick, T., Bryant, A., Egred, M., Stellos, K., Spyridopoulos, I., investigators, t.C., 2020. Effect of ciclosporin on safety, lymphocyte kinetics and left ventricular remodelling in acute myocardial infarction. Br. J. Clin. Pharmacol. 86, 1387–1397. https://doi.org/10.1111/bcn.14252
- Corp, I., IBM SPSS Statistics for Windows. 2024.
- Crapnell, R.D., Canfarotta, F., Czulak, J., Johnson, R., Betlem, K., Mecozzi, F., Down, M. P., Eersels, K., van Grinsven, B., Cleij, T.J., Law, R., Banks, C.E., Peeters, M., 2019. Thermal detection of cardiac biomarkers heart-fatty acid binding protein and ST2 using a molecularly imprinted nanoparticle-based multiplex sensor platform. ACS Sens. 4, 2838–2845. https://doi.org/10.1021/acssensors.9b01666.
- Crapnell, R.D., Dempsey-Hibbert, N.C., Peeters, M., Tridente, A., Banks, C.E., 2020. Molecularly imprinted polymer based electrochemical biosensors: overcoming the challenges of detecting vital biomarkers and speeding up diagnosis. Talanta Open 2, 100018. https://doi.org/10.1016/j.talo.2020.100018.
- Crapnell, R.D., Dempsey, N.C., Sigley, E., Tridente, A., Banks, C.E., 2022.
 Electroanalytical point-of-care detection of gold standard and emerging cardiac biomarkers for stratification and monitoring in intensive care medicine a review.
 Mikrochim. Acta 189, 142. https://doi.org/10.1007/s00604-022-05186-9.
- Cross, E., How, S., Goodacre, S., 2007. Development of acute chest pain services in the UK. Emerg. Med. J. 24, 100–102. https://doi.org/10.1136/emj.2006.043224.
- Damen, S.A.J., Cramer, G.E., Dieker, H.-J., Gehlmann, H., Ophuis, T.J.M.O., Aengevaeren, W.R.M., Fokkert, M., Verheugt, F.W.A., Suryapranata, H., Wu, A.H., van Wijk, X.M.R., Brouwer, M.A., 2020. Cardiac troponin composition characterization after non ST-Elevation myocardial infarction: relation with culprit artery, ischemic time window, and severity of injury. Clin. Chem. 67, 227–236. https://doi.org/10.1093/clinchem/hvaa231.
- Denessen, E.J.S., Nass, S.I.J., Bekers, O., Vroemen, W.H.M., Mingels, A.M.A., 2023. Circulating forms of cardiac troponin: a review with implications for clinical practice. J. Lab. Precis. Med. 8.
- Dhara, K., Mahapatra, D.R., 2020. Review on electrochemical sensing strategies for C-reactive protein and cardiac troponin I detection. Microchem. J. 156, 104857. https://doi.org/10.1016/j.microc.2020.104857.
- Erickson, H.P., 2009. Size and shape of protein molecules at the nanometer level determined by sedimentation, gel filtration, and Electron microscopy. Biol. Proced. Online 11, 32. https://doi.org/10.1007/s12575-009-9008-x.
- Eriksson, S., Ilva, T., Becker, C., Lund, J., Porela, P., Pulkki, K., Voipio-Pulkki, L.-M., Pettersson, K., 2005. Comparison of cardiac troponin I immunoassays variably affected by circulating autoantibodies. Clin. Chem. 51, 848–855. https://doi.org/ 10.1373/clinchem.2004.040089.
- Foundation, B.H., 2023a. Heart & Circulatory Disease Statistics Compendium, UK Factsheet April 2023. British Heart Foundation.
- Foundation, B.H., 2023b. Excess Deaths Involving CVD in England Since the Onset of the Covid-19 Pandemic: an Analysis and Explainer. British Heart Foundation.
- Gao, T., Zhou, Z., Cheng, D., Liu, Y., Yang, H., Wang, Y., 2024. Electrochemical biosensor for highly sensitive detection of cTn1 based on a dual signal amplification strategy of ARGET ATRP and ROP. Talanta 266, 125009. https://doi.org/10.1016/j. talanta.2023.125009.
- Gaze, D.C., Collinson, P.O., 2008. Multiple molecular forms of circulating cardiac troponin: analytical and clinical significance. Ann. Clin. Biochem. 45, 349–355.
- Geerets, B., Peeters, M., Grinsven, B.V., Bers, K., De Ceuninck, W., Wagner, P., 2013. Optimizing the thermal read-out technique for MIP-based biomimetic sensors: towards nanomolar detection limits. Sensors 13, 9148–9159. https://doi.org/ 10.1002/pssa.200983305.
- Ghilencea, L.-N., Chiru, M.-R., Stolcova, M., Spiridon, G., Manea, L.-M., Stănescu, A.-M. A., Bokhari, A., Kilic, I.D., Secco, G.G., Foin, N., Di Mario, C., 2022. Telemedicine: benefits for cardiovascular patients in the COVID-19 era. Front. Cardiovasc. Med. 9.

- Giannitsis, E., Katus, H.A., 2013. Cardiac troponin level elevations not related to acute coronary syndromes. Nat. Rev. Cardiol. 10, 623–634.
- Guidance, D., 2020. DG40. Diagnostics Assessment Committee National Institute for Health and Care Excellence. High-Sensitivity Troponin Tests for the Early Rule Out of NSTEMI NICE. https://www.nice.org.uk/guidance/DG40.
- Guy, M.J., Chen, Y.-C., Clinton, L., Zhang, H., Zhang, J., Dong, X., Xu, Q., Ayaz-Guner, S., Ge, Y., 2013. The impact of antibody selection on the detection of cardiac troponin I. Clin. Chim. Acta 420, 82–88. https://doi.org/10.1016/j.cca.2012.10.034.
- Hall, C.E., Slayter, H.S., 1959. The fibrinogen molecule: its size, shape, and mode of polymerization. J. Biophys. Biochem. Cytol. 5, 11–16. https://doi.org/10.1083/ icb.5.1.11.
- Haupt, K., Mosbach, K., 1998. Plastic antibodies: developments and applications. Trends Biotechnol. 16, 468–475. https://doi.org/10.1016/s0167-7799(98)01222-0.
- Haupt, K., Mosbach, K., 2000. Molecularly imprinted polymers and their use in biomimetic sensors. Chem. Rev. 100, 2495–2504.
- Henderson, A., 1996. Coronary heart disease: overview. Lancet. 348, S1-S4.
- Herman, D.S., Kavsak, P.A., Greene, D.N., 2017. Variability and error in cardiac troponin testing: an ACLPS critical review. Am. J. Clin. Pathol. 148, 281–295. https://doi.org/ 10.1093/ajcp/agx066.
- Hornbeck, P.V., 2015. Enzyme-linked immunosorbent assays. Curr. Protoc. Immunol. 110 (2.1.1–2.1.23).
- Katrukha, I.A., Katrukha, A.G., 2020. Myocardial injury and the release of troponins I and T in the blood of patients. Clin. Chem. 67, 124–130. https://doi.org/10.1093/clinchem/hyaa281.
- Kavsak, P.A., Roy, C., Malinowski, P., Mark, C.-T., Scott, T., Clark, L., Lamers, S., Ainsworth, C., 2018. Macrocomplexes and discordant high-sensitivity cardiac troponin concentrations. Ann. Clin. Biochem. 55, 500–504. https://doi.org/ 10.1177/0004563217734883.
- Kavsak, P.A., Kittanakom, S., 2020. Impact of switching sample types for high-sensitivity cardiac troponin I assays in the 0/1 hour algorithms. Clin. Chem. 67, 319–321. https://doi.org/10.1093/clinchem/hvaa191.
- Korff, S., Katus, H.A., Giannitsis, E., 2006. Differential diagnosis of elevated troponins. Heart 92, 987–993. https://doi.org/10.1136/hrt.2005.071282.
- Krudy, G.A., Kleerekoper, Q., Guo, X., Howarth, J.W., Solaro, R.J., Rosevear, P.R., 1994.
 NMR studies delineating spatial relationships within the cardiac troponin I-troponin C complex. J. Biol. Chem. 269, 23731–23735.
- Lippi, G., Cervellin, G., 2012. Degradation of troponin I in serum or plasma: mechanisms, and analytical and clinical implications. Semin. Thromb. Hemost. 38, 222–229. https://doi.org/10.1055/s-0032-1301419.
- Lippi, G., Cervellin, G., 2013. Choosing troponin immunoassays in a world of limited resources. J. Am. Coll. Cardiol. 62, 647–648.
- Madsen, L.H., Christensen, G., Lund, T., Serebruany, V.L., Granger, C.B., Hoen, I., Grieg, Z., Alexander, J.H., Jaffe, A.S., Van Eyk, J.E., Atar, D., 2006. Time course of degradation of cardiac troponin I in patients with acute ST-elevation myocardial infarction: the ASSENT-2 troponin substudy. Circ. Res. 99, 1141–1147. https://doi.org/10.1161/01.RES.0000249531.23654.e1.
- Mair, J., Puschendorf, B., Michel, G., 1994. Clinical significance of cardiac contractile proteins for the diagnosis of myocardial injury. In: Spiegel, H.E. (Ed.), Adv. Clin. Chem. Elsevier, pp. 63–98.
- McClements, J., Seumo Tchekwagep, P.M., Vilela Strapazon, A.L., Canfarotta, F., Thomson, A., Czulak, J., Johnson, R.E., Novakovic, K., Losada-Pérez, P., Zaman, A., Spyridopoulos, I., Crapnell, R.D., Banks, C.E., Peeters, M., 2021. Immobilization of molecularly imprinted polymer nanoparticles onto surfaces using different strategies: evaluating the influence of the functionalized interface on the performance of a thermal assay for the detection of the cardiac biomarker troponin I. ACS Appl. Mater. Interfaces 13, 27868–27879. https://doi.org/10.1021/
- McClements, J., Bar, L., Singla, P., Canfarotta, F., Thomson, A., Czulak, J., Johnson, R.E., Crapnell, R.D., Banks, C.E., Payne, B., Seyedin, S., Losada-Pérez, P., Peeters, M., 2022. Molecularly imprinted polymer nanoparticles enable rapid, reliable, and robust point-of-care thermal detection of SARS-CoV-2. ACS Sens. 7, 1122–1131. https://doi.org/10.1021/acssensors.2c00100.
- Morjana, N.A., 1998. Degradation of human cardiac troponin I after myocardial infarction. Biotechnol. Appl. Biochem. 28, 105–111.
- Mostafa, A.M., Barton, S.J., Wren, S.P., Barker, J., 2021. Review on molecularly imprinted polymers with a focus on their application to the analysis of protein biomarkers. TrAC, Trends Anal. Chem. 144, 116431. https://doi.org/10.1016/j. trac.2021.116431.
- Nadarajah, R., Farooq, M., Raveendra, K., Nakao, Y.M., Nakao, K., Wilkinson, C., Wu, J., Gale, C.P., 2023. Inequalities in care delivery and outcomes for myocardial infarction, heart failure, atrial fibrillation, and aortic stenosis in the United Kingdom. Lancet Reg. Health Eur. 33. https://doi.org/10.1016/j.lanepe.2023.100719.
- Ojha, N., Dhamoon, A.S., 2023. Myocardial infarction, in StatPearls. Treasure Island (FL).
- Ostrovidov, S., Ramalingam, M., Bae, H., Orive, G., Fujie, T., Hori, T., Nashimoto, Y., Shi, X., Kaji, H., 2023. Molecularly imprinted polymer-based sensors for the detection of Skeletal- and cardiac-muscle-related analytes. Sensors 23, 5625.
- Park, K.C., Gaze, D.C., Collinson, P.O., Marber, M.S., 2017. Cardiac troponins: from myocardial infarction to chronic disease. Cardiovasc. Res. 113, 1708–1718.
- Pickering, J.W., Than, M.P., Cullen, L., Aldous, S., Ter Avest, E., Body, R., Carlton, E.W., Collinson, P., Dupuy, A.M., Ekelund, U., 2017. Rapid rule-out of acute myocardial infarction with a single high-sensitivity cardiac troponin T measurement below the limit of detection: a collaborative meta-analysis. Ann. Intern. Med. 166, 715–724.
- Potter, J.M., Hickman, P.E., Cullen, L., 2022. Troponins in myocardial infarction and injury. Aust. Prescr. 45, 53–57. https://doi.org/10.18773/austprescr.2022.006.

- Regan, B., Boyle, F., O'Kennedy, R., Collins, D., 2019. Evaluation of molecularly imprinted polymers for point-of-care testing for cardiovascular disease. Sensors 19, 2007.
- Roberto de Oliveira, P., Crapnell, R.D., Garcia-Miranda Ferrari, A., Wuamprakhon, P., Hurst, N.J., Dempsey-Hibbert, N.C., Sawangphruk, M., Campos Janegitz, B., Banks, C.E., 2023. Low-cost, facile droplet modification of screen-printed arrays for internally validated electrochemical detection of serum procalcitonin. Biosens. Bioelectron. 228, 115220. https://doi.org/10.1016/j.bios.2023.115220.
- Sacco, R.L., Kasner, S.E., Broderick, J.P., Caplan, L.R., Connors, J., Culebras, A., Elkind, M.S., George, M.G., Hamdan, A.D., Higashida, R.T., 2013. An updated definition of stroke for the 21st century: a statement for healthcare professionals from the American heart association/american stroke association. Stroke 44, 2064–2089.
- Sakamoto, S., Putalun, W., Vimolmangkang, S., Phoolcharoen, W., Shoyama, Y., Tanaka, H., Morimoto, S., 2018. Enzyme-linked immunosorbent assay for the quantitative/qualitative analysis of plant secondary metabolites. J. Nat. Med. 72, 32–42. https://doi.org/10.1007/s11418-017-1144-z.
- Saleh, M., Ambrose, J.A., 2018. Understanding myocardial infarction. F1000Res 7. https://doi.org/10.12688/f1000research.15096.1.
- Sarvutiene, J., Prentice, U., Ramanavicius, S., Ramanavicius, A., 2024. Molecular imprinting technology for biomedical applications. Biotechnol. Adv. 71, 108318. https://doi.org/10.1016/j.biotechadv.2024.108318.
- Sengupta, S., Biswal, S., Titus, J., Burman, A., Reddy, K., Fulwani, M.C., Khan, A., Deshpande, N., Shrivastava, S., Yanamala, N., Sengupta, P.P., 2023. A novel breakthrough in wrist-worn transdermal troponin-I-sensor assessment for acute myocardial infarction. Eur. Heart. J. Digit. Health. 4, 145–154. https://doi.org/10.1093/ehjdh/ztad015.
- Sharma, S., Jackson, P., Makan, J., 2004. Cardiac troponins, 57. BMJ Publishing Group, pp. 1025–1026.
- Shumyantseva, V.V., Bulko, T.V., Sigolaeva, L.V., Kuzikov, A.V., Pogodin, P.V., Archakov, A.I., 2018. Molecular imprinting coupled with electrochemical analysis for plasma samples classification in acute myocardial infarction diagnostic. Biosens. Bioelectron. 99, 216–222. https://doi.org/10.1016/j.bios.2017.07.026.
- Stepinska, J., Lettino, M., Ahrens, I., Bueno, H., Garcia-Castrillo, L., Khoury, A., Lancellotti, P., Mueller, C., Muenzel, T., Oleksiak, A., Petrino, R., Guimenez, M.R., Zahger, D., Vrints, C.J.M., Halvorsen, S., de Maria, E., Lip, G.Y.H., Rossini, R., Claeys, M., Huber, K., 2020. Diagnosis and risk stratification of chest pain patients in the emergency department: focus on acute coronary syndromes. A position paper of the acute cardiovascular care association. Eur. Heart J. Acute Cardiovas. Care 9, 76-89. https://doi.org/10.1177/2048872619885346.
- Thomas, C., Brennan, A., Goka, E., Squires, H.Y., Brenner, G., Bagguley, D., Buckley Woods, H., Gillett, M., Leaviss, J., Clowes, M., Heathcote, L., Cooper, K., Breeze, P., 2020. What are the cost-savings and health benefits of improving detection and management for six high cardiovascular risk conditions in England? An economic evaluation. BMJ Open 10, e037486. https://doi.org/10.1136/bmjopen-2020-037486.
- van Grinsven, B., Vandenryt, T., Duchateau, S., Gaulke, A., Grieten, L., Thoelen, R., Ingebrandt, S., De Ceuninck, W., Wagner, P., 2010. Customized impedance spectroscopy device as possible sensor platform for biosensor applications. Phys. Stat. Sol. (a) 207–919-923
- van Grinsven, B., Eersels, K., Peeters, M., Losada-Pérez, P., Vandenryt, T., Cleij, T.J., Wagner, P., 2014. The heat-transfer method: a versatile low-cost, label-free, fast, and user-friendly readout platform for biosensor applications. ACS Appl. Mater. Interfaces 6, 13309–13318. https://doi.org/10.1021/am503667s.
- Vasapollo, G., Sole, R.D., Mergola, L., Lazzoi, M.R., Scardino, A., Scorrano, S., Mele, G., 2011. Molecularly imprinted polymers: present and future prospective. Int. J. Mol. Sci. 12, 5908–5945.
- Vignoli, A., Tenori, L., Morsiani, C., Turano, P., Capri, M., Luchinat, C., 2022. Serum or plasma (and which plasma), that is the question. J. Proteome Res. 21, 1061–1072. https://doi.org/10.1021/acs.jproteome.1c00935.
- Vylegzhanina, A.V., Kogan, A.E., Katrukha, I.A., Koshkina, E.V., Bereznikova, A.V., Filatov, V.L., Bloshchitsyna, M.N., Bogomolova, A.P., Katrukha, A.G., 2019. Full-size and partially truncated cardiac troponin complexes in the blood of patients with acute myocardial infarction. Clin. Chem. 65, 882–892. https://doi.org/10.1373/clinchem.2018.301127.
- Wang, H., Yao, C., Fan, J., He, Y., Wang, Z., 2023. One-pot synthesis of AuPt@FexOy nanoparticles with excellent peroxidase-like activity for development of ultrasensitive colorimetric lateral flow immunoassay of cardiac troponin I. Biosens. Bioelectron. 237, 115508. https://doi.org/10.1016/j.bios.2023.115508.
- Wilkins, E., Wilson, L., Wickramasinghe, K., Bhatnagar, P., Leal, J., Luengo-Fernandez, R., Burns, R., Rayner, M., Townsend, N., 2017. European cardiovascular disease statistics 2017. European Cardiovascular Disease Statistics.
- Wu, A.H.B., Feng, Y.-J., Moore, R., Apple, F.S., McPherson, P.H., Buechler, K.F., Bodor, G., for, f.t.A.A., Standardization, C.C.S.o.c., 1998. Characterization of cardiac troponin subunit release into serum after acute myocardial infarction and comparison of assays for troponin T and I. Clin. Chem. 44, 1198–1208. https://doi. org/10.1093/clinchem/44.6.1198.
- Xie, Y., Xu, E., Bowe, B., Al-Aly, Z., 2022. Long-term cardiovascular outcomes of COVID-19. Nat. Med. 28, 583–590. https://doi.org/10.1038/s41591-022-01689-3.
- Zhan, T., Su, Y., Lai, W., Chen, Z., Zhang, C., 2022a. A dry chemistry-based ultrasensitive electrochemiluminescence immunosensor for sample-to-answer detection of cardiac

troponin I. Biosens. Bioelectron. 214, 114494. https://doi.org/10.1016/j. bios. 2022.114494

Zhan, T., Su, Y., Lai, W., Chen, Z., Zhang, C., 2022b. A dry chemistry-based ultrasensitive electrochemiluminescence immunosensor for sample-to-answer detection of cardiac troponin I. Biosens. Bioelectron. 214, 114494. https://doi.org/10.1016/j.bios.2022.114494.

Zhou, J., Wu, R., Williams, C., Emberson, J., Reith, C., Keech, A., Robson, J., Wilkinson, K., Armitage, J., Gray, A., Simes, J., Baigent, C., Mihaylova, B., 2023. Prediction models for individual-level healthcare costs associated with cardiovascular events in the UK. Pharmacoeconomics 41, 547–559. https://doi.org/10.1007/s40273-022-01219-6.